

HYSTERETIC CONTROLLED CLASS F3 AMPLIFIER SYSTEM WITH REDUCED THD WITH IMPROVED TIME RESPONSE

G Padmanabha Sivakumar¹ and Umapathy Kannan²

¹Research Scholar, ² Associate Professor,

¹Department of Electronics and Instrumentation Engineering,

²Department of Electronics and Communication Engineering,

¹Sri Chandrasekharendra Saraswathi Viswa Mahavidyalaya, Kanchipuram, Tamilnadu, India

¹gpskumar@kanchiuniv.ac.in, ²umapathykannan@gmail.com

Abstract—Class F3 amplifier circuit is a good interface between semi converter and induction heater. The aim of this work is to improve the dynamic response of closed loop-controlled class F3 based IH system. Circuit modeling and simulation analysis of hysteretic controlled class F3 based induction heating system described in the paper. Class F3 amplifier is suggested in the present work to generate quick heat in the induction cooker. Class F3 amplifier is a simple system with single switch and reactive elements. The class F3 amplifier produces high frequency currents required by the load. Closed loop system with and without hysteretic element are simulated and the corresponding results are presented. The results of comparative study are presented to show the reduction in current ripple. The time domain parameters and the THD content are also improved. The hardware is engineered and the test results are presented. A simple hysteretic control is applied to Induction heating system. The results indicate that the output current THD is reduced by using the hysteretic controller.

Keywords—Induction heating (IH), power amplifier (PA), class-f amplifier, hysteretic controller.

I. INTRODUCTION

There is a need for quick heating in domestic applications. This paper explores the possibility of using class F3 amplifier for induction heating. RF Microwave power amplifier with improved efficiency is given by Gao [1-2]. Improved design technique of a broadband class E power amplifier is given by Qin [3]. The superior ways to design RF-PA design are given by Cripps [4]. Class B/F amplifiers with improved efficiency, effect of harmonics and working of PHEMET device is given by White [5]. A method to measure harmonics in load is given by Colantonio [6]. Various circuit topologies for base station application is given by Akkul, Roberts walker and Bosch [7]. New design technique for improving efficiency of Class-F PA is given by Ooi [8].

Improved efficiency for class F MMIC PA's of KU-band is given by Ozalas [9]. SiGe based IGBT Class-F PA with full integration is given by Oscullivan [10]. New control methods and considerations for tuning of Class E/F amplifiers is given by S. Zerouali [11]. The entire research on the design of Class-D/ Class-E/ Class-F amplifier systems is focused on the improvement of efficiency and other characteristics.

The above literature does not deal with hysteretic controlled class-F3 induction heater system. This work proposes hysteretic control for class F3 amplifier system. The performance of the closed loop system with and without hysteretic controlled are presented. The Section-II deals with disruption of existing and proposed system. Section-III deals with simulation analysis, observations and hardware results. The work is concluded in the section-IV.

II. BENEFITS OF DIGITAL BACK PROPAGATION

A. Existing system with Class-E amplifier:

This section describes the existing system of Class E Amplifier based Induction Heating System (CEIH), which is shown in the Fig.1. DC is transformed into high frequency AC with help of class-E amplifier.

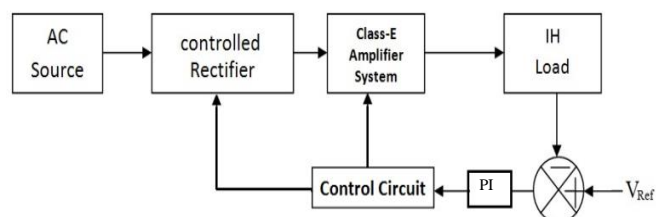


Fig. 1 Block diagram of the existing IH system

Generated heat is produced due to eddy current losses. Regulating the output voltage is obtained using the PI controller.

B. Hysteretic controlled closed loop Class-F3 Amplifier system:

Hysteretic controlled closed loop Class-F3 Amplifier Induction Heating system (HCCFAIHS) is proposed to overcome CEIH is shown in Fig.2. Low frequency AC is changed into DC with help of the controlled rectifier. The output of the rectifier is manifested into high frequency AC using the class F3 amplifier. Class-E amplifier is replaced by ClassF3 amplifier and PI controller is replaced by hysteretic controller to improve the dynamic response.

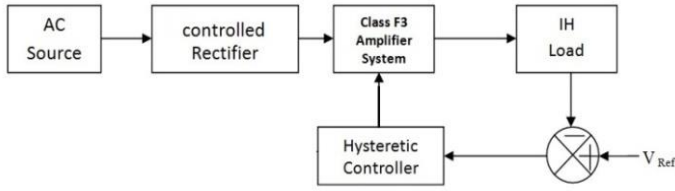


Fig. 2 Block diagram of the proposed IH system.

C. Analysis of CFAIHS:

Design calculations are performed using the following equations:

V_d - DC input voltage; L_r -Inductance of Class-F amplifier; C_r -Capacitance of Class-F amplifier; T_r -Rise time; T_p -Peak time; E_{ss} - Steady State error; C_1 - Filter Capacitor.

$$I = V_d \sqrt{C_r/L_r} e^{-\alpha t} \sin \omega t \quad (1)$$

The voltage across the capacitor is

$$V = V_d (1 - \cos \omega t) \quad (2)$$

ZVS period of CFAIH system is calculated using equation (2).

$$r = \frac{1}{4\sqrt{3}fCR} \quad (3)$$

The value of filter capacitor is determined using the expression for ripple factor given in equation (3).

III. SIMULATION RESULTS

Class-F3 amplifier induction heating system (CFAIHS) without hysteretic controller is provided in Fig.3. Load voltage is sensed and it is compared with the reference voltage. The voltage error is applied to a PI controller. The output voltage of PI controller is given to two comparators. Pulse width is selected based on the error. The input current is shown in Fig.4. The output

Current is given in the Fig.5. The spectrum for current is shown in Fig.6 and the THD is 4.6%. The applied voltage at the input is shown in Fig.7 and its value increases from 25V to 30V. The output voltage of the system is shown in the Fig 8. The power obtained at the output is shown in Fig.9 and its value is 80 W.

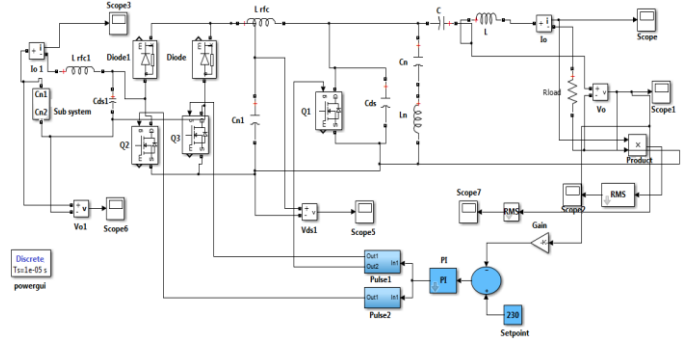


Fig. 3 CFAIHS without hysteretic controller

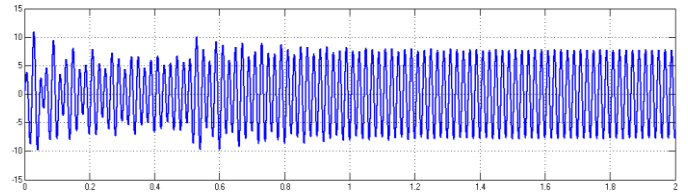


Fig. 4 Input current to CFAIHS without hysteretic controller.

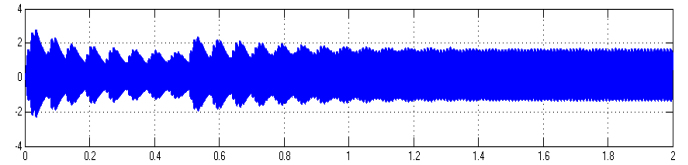


Fig. 5 Output current from CFAIHS without hysteretic controller.

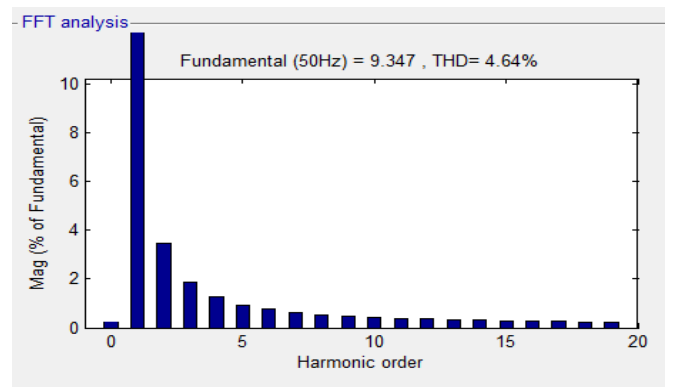


Fig. 6 Current spectrum of CFAIHS without hysteretic controller.

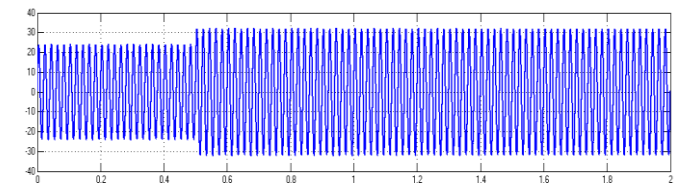


Fig. 7 Input voltage to CFAIHS without hysteretic controller.

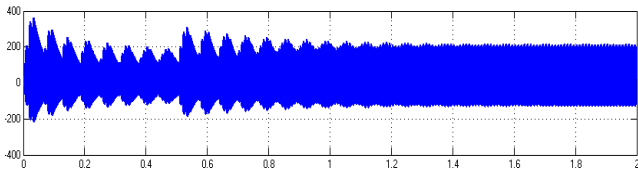


Fig. 8 Output voltage of CFAIHS without hysteretic controller.

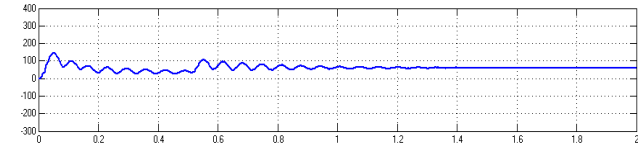


Fig. 9 Output power of CFAIHS without hysteretic controller.

The CFAIHS system with hysteretic controller is designed to ensure proper regulation of the output voltage and output current. It is shown in the Fig.10. A hysteretic element is included before the pulse generator. The current applied at the input is given in Fig.11. Output current is shown in Fig.12. The input and output voltage are given in the Fig 13, Fig 14 respectively The spectrum for current is shown in Fig.15 and THD content is 1.48%.. The output power is shown in Fig.16 and its value is 70 W.

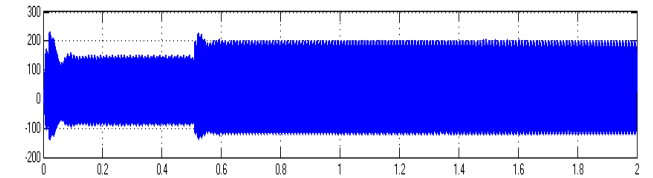


Fig. 14 Output voltage to CFAIHS with hysteretic controller

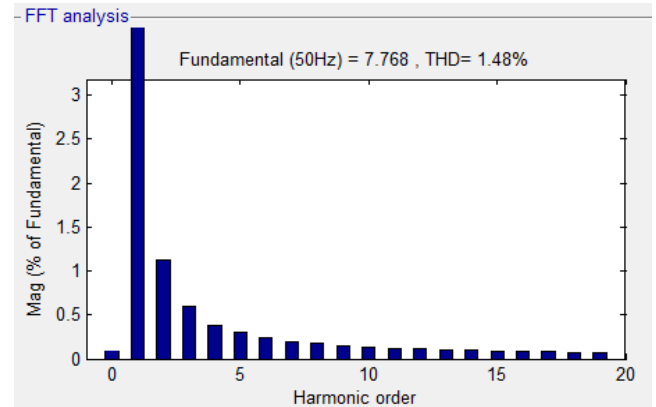


Fig. 15 Current spectrum of CFAIHS with hysteretic controller

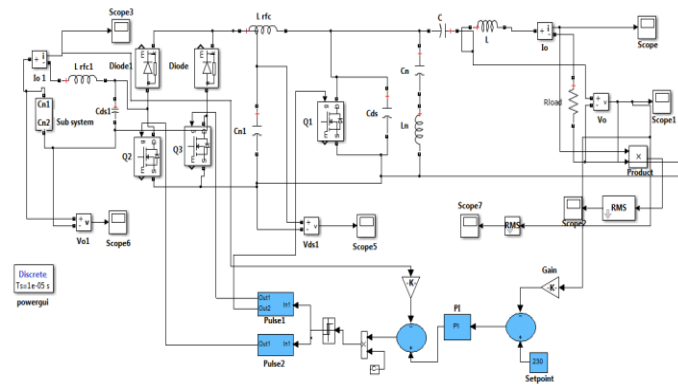


Fig. 10 CFAIHS with hysteretic controller.

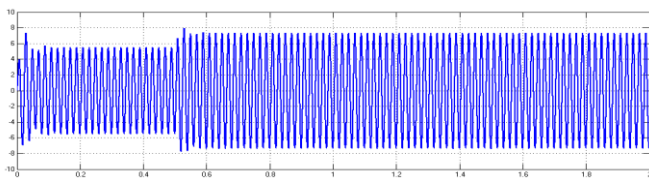


Fig. 11 Input current to CFAIHS with hysteretic controller.

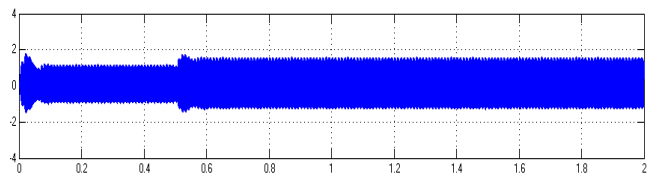


Fig. 12 Output current of CFAIHS with hysteretic controller.

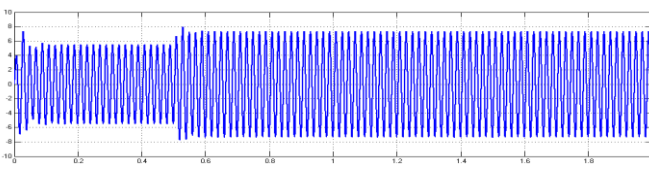


Fig. 13 Input voltage to CFAIHS with hysteretic controller.

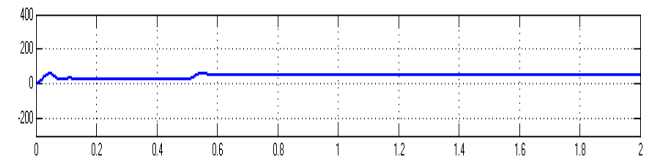


Fig. 16 Output power of CFAIHS with hysteretic controller

The simulation studies on HC-CFAIHS are done for different reference values of voltage. The comparison of time domain parameters for reference values of 180V, 200V and 230V are presented in the Table-1, Table-2 and Table- 3 respectively.

Table: 1

Comparison of Time domain parameters (Vref=180v)

Controller Type	t_r	t_s	t_p	e_{ss}
PI	0.067	0.98	0.63	2.8
Hysteretic	0.56	0.63	0.53	1.7

Table: 2

Comparison of Time domain parameters (Vref=200v)

Controller Type	t_r	t_s	t_p	e_{ss}
PI	0.066	0.96	0.62	2.6
Hysteretic	0.54	0.61	0.51	1.5

Table: 3

Comparison of Time domain parameters (Vref=180v)

Controller Type	t_r	t_s	t_p	e_{ss}
PI	0.065	0.95	0.59	2.4
Hysteretic	0.53	0.6	0.5	1.4

The settling time reduces from 0.53s to 0.50s as the reference voltage value increases from 180V to 230V. The steady state error decreases from 1.7V to 1.4V. Thus

the steady state error and settling time values decrease with the increase in the reference value. The comparison of current THD is shown in Table-4. The THD with PI Controller is 4.4% and THD with hysteretic controller is 1.48%. The THD with hysteretic controller is reduced by 1.2%. Thus, it clearly shows that the performance of IH system with hysteretic controller is superior to the system without hysteretic.

Table: 4
Comparison of THD

Controller Type	Output Current THD
PI	4.64%
Hysteretic	1.48%

The PIC controlled hardware for class F3 system is constructed and examined. The snapshot of fabricated hardware is provided in Fig 17. The hardware consists of control board, rectifier board and Class F Amplifier (CFA) board. AC input voltage applied to the rectifier is shown in Fig 18. The output of the uncontrolled rectifier is given in Fig 5.2. The switching pulses produced by PIC are provided in Fig 5.3 and the amplitude of this pulse is 5V. The output of the pulse amplifier increases the amplitude of pulse to 10V. The output of the amplifier shown in Fig 20. The output voltage of the class F3 amplifier is shown in Fig 21. This figure matches with Fig 14. Therefore experimental results are similar to simulation results. The parameter details used for hard-ware and software mentioned in the Table.5.

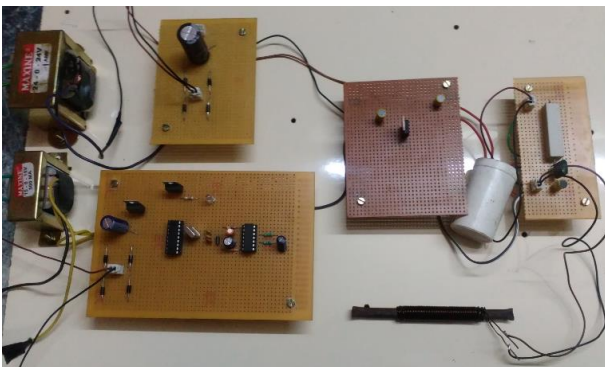


Fig. 17 Fabricated hardware of class F3 amplifier system

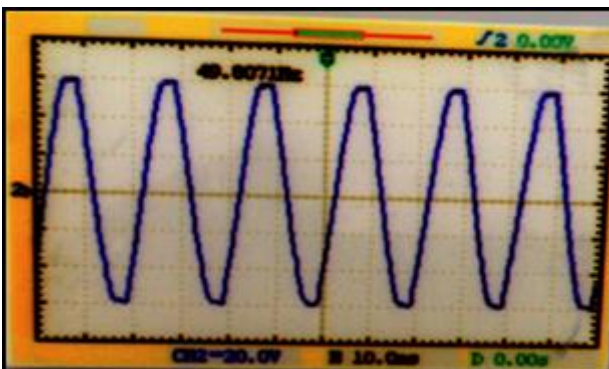


Fig. 18 AC input voltage to the rectifier of the CFA system.

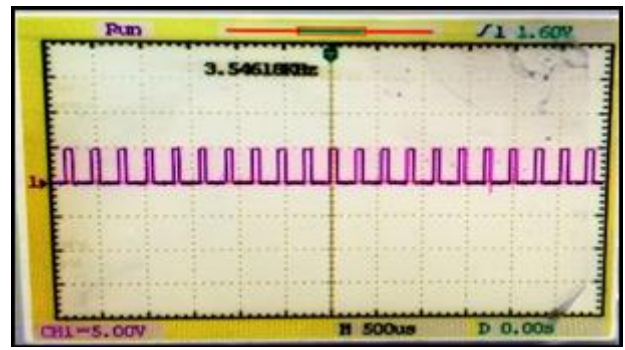


Fig. 19 Switching pulses of PIC microcontroller.

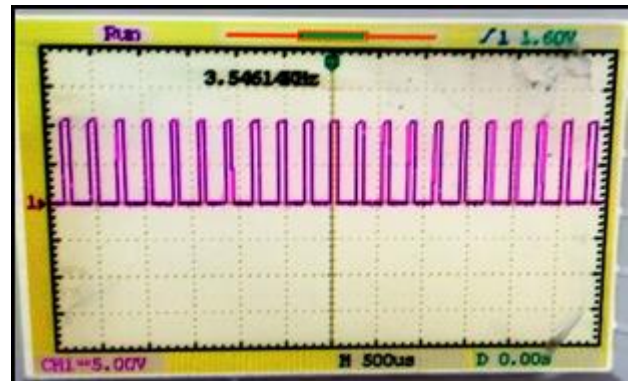


Fig. 20 The output of the pulse amplifier

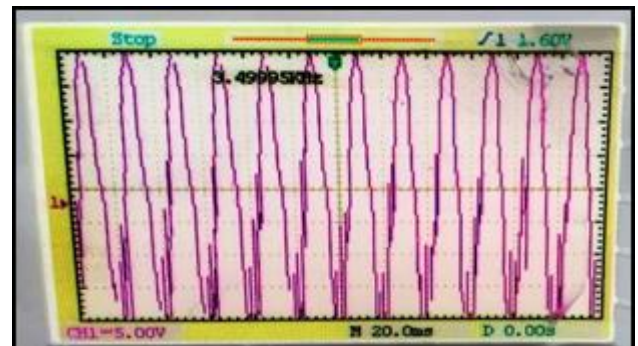


Fig. 21 Output voltage of class F3 amplifier.

Table: 5
System simulation parameters

Parameters	Simulation Value	Hardware Value
Vd	24v	24v
L1	0.5 μ H	0.8 μ H
L2	1 μ H	1.5 μ H
Cr	4.2 μ F	5 μ F
C1	2200 μ F	2200 μ F
MOSFET	500V/8A	500V/8A
Diode	230V/1A	230V/1A

The detailed total hardware diagram of the Class-F amplifier based Induction heating system is shown in the Figure.22 below.

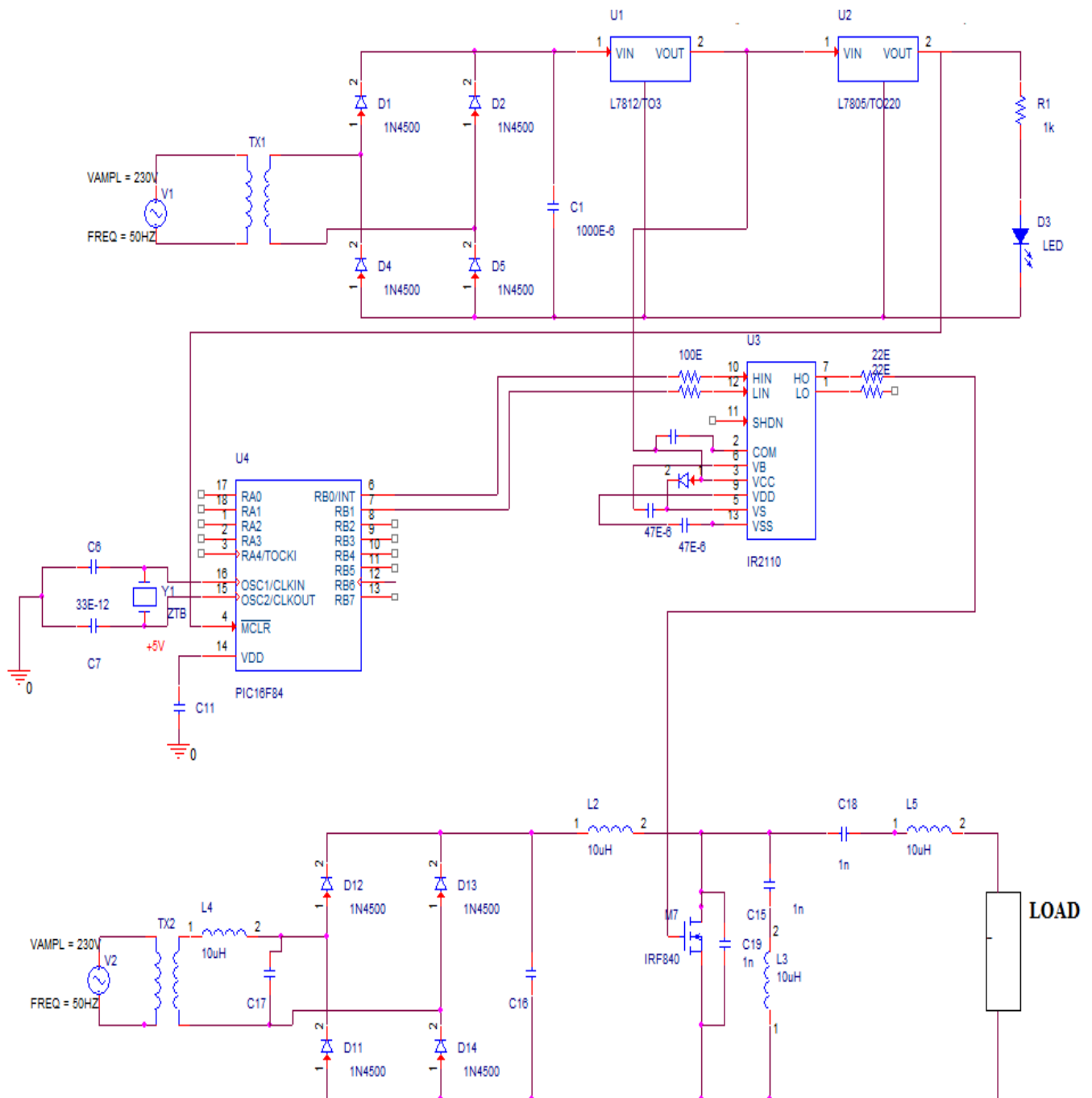


Fig. 22 Hardware Connection diagram of class F3 amplifier induction heating system.

IV. CONCLUSION

In this paper, Class F3 amplifier system was successfully designed; modeled & simulated using MATLAB and the results of case studies with and without hysteretic control system were presented. The induction heater load was shown as series combination of resistance and inductance. It was observed that THD content is reduced from 4.6% to 1.4% by adding hysteretic controller. The settling time was reduced to 0.6 sec using hysteretic controller. The steady state error in the output voltage was reduced from 2.4V to 1.4V by introducing Hysteretic controller. The results in this paper are clear indication of improvement in dynamic response. The experimental module is implemented to validate the simulation results. The benefits of ClassF3 system are mini-mum switching losses, less switching stress and high-power density.

The disadvantages of Class F3 system is that frequency cannot be varied by wide range. The scope of this work was the modeling and simulation of ClassF3 amplifier with hysteretic control. The comparison with ANN controlled system will be done in future.

References

- [1] S. Gao, (2006) High-efficiency class-F RF/Microwave power amplifiers, IEEE Microwave Magazine, vol. 7, no. 1, pp. 40-48.
- [2] S. Gao, P. Butterworth, S. Ooi, and A. Sambell,(2006) High efficiency class-F power amplifier design including

- [3] input harmonic termination, IEEE Microwave and Wireless Components Letters, vol. 16, no. 2, pp. 81-83.
- [4] Y. Qin, S. Gao and A. Sambell, (2005) "Improved design technique of a broadband class-E power amplifier at 2GHz," in Proc. European Microwave Conf 2005, Paris, pp. 453-457.
- [5] S. Cripps, "Advanced techniques in RF power amplifier design", Artech House, 2002.
- [6] P. M. White, (1998) "Effect of input harmonic terminations on high efficiency class-B and class-F operation of PHEMT devices," IEEE Int. Microwave Symp. Dig., pp. 1611-1614.
- [7] P. Colantonio, F. Giannini, E. Limiti, and V. Teppati, (2004) An approach to harmonic load- and source-pull measurements for high-efficiency PA design, IEEE Trans. Microw. Theory Tech., Vol. 52, pp. 191-198.
- [8] M. Akkul, M. Roberts, V. Walker, and W. Bosch,(2004) High efficiency power amplifier input/output circuit topologies for base station and WLAN applications, IEEE Int. Microwave Symp. Dig., pp. 843-846.
- [9] S. Ooi, S. Gao, A. Sambell, and D. Smith, (2004) High efficiency Class-F power amplifier design technique, Microwave Journal, vol. 47, no.11, pp.110- 122 .
- [10] M. Ozalas (2005), High-efficiency class-F MMIC power amplifiers" at Ku-band, <http://www.mitre.org>.
- [11] J. OSullivan, et al.,(2003), A fully integrated high efficiency SiGe HBT class F power am-plifier at 2.2 GHz", in IEEE High Frequency Postgraduate Student Colloquium, pp. 48-51.
- [12] S. Zerouali, A. Hadri Hamida, S. M. Mimoune, A. Allag and A. Bensalem (2013) "Adap-tive control with tuning function control design applied to class-E/F inverter," 2013 3rd In-ternational Conference on Electric Power and Energy Conversion Systems, Istanbul, pp. 1-6.